

ADVANCED TRANSVERSE INTEGRATION FOR THE METHOD OF CHARACTERISTICS

François Févotte, Simone Santandrea and Richard Sanchez

Commissariat à l'Énergie Atomique

Centre de Saclay

CEA/DEN/DANS/DM2S/SERMA/LTSD

francois.fevotte@cea.fr, simone.santandrea@cea.fr, richard.sanchez@cea.fr

ABSTRACT

A novel technique for a better computation of transmission probabilities has been developed for the method of characteristics in unstructured meshes (MOC). This technique relies on a transverse quadrature that properly accounts for discontinuities along trajectories, without penalizing the transverse step, and on the use of a Taylor expansion for the transverse integration of the transmission probability. The implementation of this new technique has proved rather successful, insofar as the method requires a much larger tracking step (up to five times) than the regular MOC to obtain a given accuracy for the reaction rates.

Key Words: Method of Characteristics, Tracking, Transverse integration

1. INTRODUCTION

In the past years, the Method of Characteristics (MOC) has become a popular tool for the numerical solution of the neutron transport equation [2, 3, 5, 6]. The MOC accurately accounts for transport within the regions by means of an analytical integration of the neutron flux along a set of trajectories in directions given by an angular quadrature formula. In most practical applications of the MOC a (constant step) mesh is defined over the plane transverse to the direction of propagation Ω and the assumption is made that the angular flux is constant across each mesh cell: $\psi(\mathbf{r}_\perp + x\Omega, \Omega) = \psi_k(x, \Omega)$ for $\mathbf{r}_\perp \in I_k$, where I_k is the k 'th transverse mesh cell. Moreover, the transmission of the constant flux ψ_k across one region intersecting the trajectory band within the transverse mesh cell I_k is approximated by the value of the transmission for the trajectory at the center of the mesh cell. This situation is illustrated in Fig. 1 for the case of XY two-dimensional geometries for which there is only one transverse coordinate x_\perp .

Hence, two approximations affect the precision of the calculation in terms of the transverse quadrature step Δ : a) the introduction of a piecewise constant transverse flux approximation and b) the calculation of the transmission probability using the middle trajectory of the mesh interval. These approximations are akin to using a constant step (rectangular) quadrature on \mathbf{r}_\perp . A further source of error results from the presence of regions that partially intersect a trajectory band. Numerically, the intersection occurs only when the middle trajectory intersects the region. For example, for the trajectory band I_{k-1} in Fig. 1, the effect of the partially inserted region is not accounted for and transmission is computed as if the inserted region was not there. This not only affects the precision of the calculation but also results in a non uniform convergence with the quadrature step Δ . As a consequence of these approximations, a rather small tracking step Δ has to be used in order to obtain accurate results with the MOC.

To eliminate the oscillations and achieve uniform convergence one can project all the material

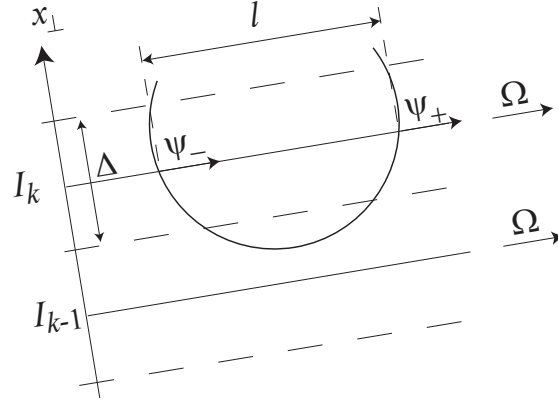


Figure 1. Illustration for MOC transverse integration. The transverse current $\Delta \times \psi_-$ entering the region produces the transverse current $\Delta \times \psi_+$ exiting the region. The transmitted flux $\psi_+ = e^{-\Sigma l} \times \psi_-$ is computed using the track length l of the middle trajectory.

discontinuities over the transverse direction and integrate within each two consecutive projections. Moreover, because the integrand is now continuous, the latter integration can be done using a more accurate Gauss-Legendre (GL) quadrature [4]. Unfortunately, the projection of discontinuities usually produces a transverse mesh with a large number of small mesh cells that, not only do not require GL quadrature, but that is too precise and onerous for routine applications. Even when limiting the projection of discontinuities to each cell of an assembly, there is no notable advantage on using a GL quadrature [7]. Besides, this latter solution introduces a fair amount of numerical dispersion for the transverse flux when passing from one cell to the following.

In this work we propose a new tracking technique that a) uses a Taylor expansion to improve on the calculation of the transmission probability and b) uses macrobands to locally project the discontinuities so as to minimize the presence of very small quadrature steps. The paper is organized as follows: In the next section we give a brief description of the method of characteristics. In Section 3 we present the new macroband tracking technique, while numerical examples are given in the following section. We end with a brief conclusion. In the Appendix we outline the extension of macroband tracking to the case of closed domains with cyclic trajectories.

2. THE METHOD OF CHARACTERISTICS

The method of characteristics provides a solution for the transport equation in a geometric domain D composed of unstructured homogeneous cells:

$$\begin{cases} (\mathbf{\Omega} \cdot \nabla + \Sigma)\psi = q, & (\mathbf{r}, \mathbf{\Omega}) \in D \times (4\pi) \\ \psi = \beta \psi + \psi_0, & (\mathbf{r}, \mathbf{\Omega}) \in \partial D \times (2\pi)_- \end{cases} \quad (1)$$

where $\psi(\mathbf{r}, \mathbf{\Omega})$ represents the angular flux at position \mathbf{r} in direction $\mathbf{\Omega}$, $\Sigma(\mathbf{r})$ represents the total cross-section and $q(\mathbf{r}, \mathbf{\Omega})$ is the emission density. β is an albedo operator on the domain boundary and ψ_0 represents an angular flux entering through the boundary.

The MOC equations are based on the discrete ordinate formulation of the transport equation (1). The spatial discretization is achieved by introducing approximated representations for the fluxes within the regions and for the fluxes on the regions boundaries. First, a flat spatial representation for the source term is used within each region:

$$q(\mathbf{r}) = q_i, \quad \mathbf{r} \in \text{region } i \quad (2)$$

Second, a direction-dependent, piecewise constant approximation is used for the angular fluxes over the regions boundaries. This representation is obtained by defining a mesh $\{I_k, k = 1, \dots, K\}$ over the transverse coordinates and by assuming that the angular flux is constant across each mesh cell:

$$\psi(\mathbf{r}, \boldsymbol{\Omega}) = \psi_k(x, \boldsymbol{\Omega}), \quad \mathbf{r}_\perp \in I_k, \quad (3)$$

where $\mathbf{r} = \mathbf{r}_\perp + x \boldsymbol{\Omega}$.

The MOC is based on two equations [1]: the transmission equation (4) and the balance equation. The latter does not concern us in this work. The transmission equation describes the relation between the incoming and exiting angular fluxes and the internal source of the region: from cell homogeneity and the assumption of flat source (2):

$$\psi_t^+(\boldsymbol{\Omega}) = e^{-\Sigma R(t)} \psi_t^-(\boldsymbol{\Omega}) + \frac{1 - e^{-\Sigma R(t)}}{\Sigma} q(\boldsymbol{\Omega}), \quad (4)$$

where t denotes a trajectory of direction $\boldsymbol{\Omega}$ crossing a region of total cross section Σ , the $\psi_t^\pm(\boldsymbol{\Omega})$ are the angular fluxes exiting (+) and entering (-) the region along the trajectory, $R(t)$ is the chord length of the trajectory within the region and $q(\boldsymbol{\Omega})$ is the flat angular source term in the region.

For consistency with the piecewise constant approximation for the angular flux on the transverse plane, the above equation should be averaged over all trajectories in the trajectory band defined by the transverse mesh cell I_k . The result is

$$\psi_k^+(\boldsymbol{\Omega}) = T \psi_k^-(\boldsymbol{\Omega}) + \frac{1 - T}{\Sigma} q(\boldsymbol{\Omega}), \quad (5)$$

where $\psi_k^\pm(\boldsymbol{\Omega})$ are the transverse averaged values of the boundary fluxes and

$$T = \frac{\int_{I_k} e^{-\Sigma R(\mathbf{r}_\perp)} d\mathbf{r}_\perp}{\int_{I_k} d\mathbf{r}_\perp} \quad (6)$$

is the transverse averaged transmission. In this last equation, $R(\mathbf{r}_\perp) = R(t)$ is the chord length within the region for the trajectory t through \mathbf{r}_\perp .

However, instead of using the consistent value (6), in the classical MOC one uses the approximation

$$T \sim \exp(-\Sigma R_k), \quad (7)$$

where R_k is the chord length for the trajectory through the center of transverse cell I_k . Note that this technique is only exact for the extreme case when the intersections of the trajectories with the region are of equal length. The error introduced by this approximation is thought to be partially compensated by direction-dependent chord length renormalization [4].

To palliate the impact of this approximation is the main aim of our work.

3. A NEW TRACKING METHOD FOR THE CHARACTERISTICS

In our work we have chosen to use a semi-analytical approximation for the true transmission in (6). The details will be given for the case of XY two-dimensional geometries, for which there is only a transverse coordinate x_{\perp} . For this discussion we shall assume that the region is fully intersected by the trajectory band defined by a mesh cell I_k and will discuss later a technique to avoid region discontinuities. One may think of these trajectory bands as 'homogeneous' bands, i.e., as bands composed of homogeneous sections.

We note that if the region boundaries are straight lines, then the calculation of T in (6) can be done analytically to obtain

$$T = \frac{e^{-\Sigma R_k}}{\Sigma a_k} \sinh(\Sigma a_k).$$

Here $a_k = \Delta(\tan \alpha_+ - \tan \alpha_-)/2$, where Δ is the mesh cell width and α_{\pm} are the angles of the upstream (-) and downstream (+) boundaries of the cell with respect to the transverse direction. This is an attractive result in that it yields the exact transmission while requiring the storage of two parameters, R_k and a_k , per track and the evaluation of two functions per track sweep. Unfortunately, for curved surfaces, such as arcs of circles, there is no analytical expression for T , that now contains an integral over φ involving the exponential $\exp[-\Sigma f(\varphi)]$, where $f(\varphi)$ is a non linear function of φ .

Because for homogenous bands there are no discontinuities within the trajectories path, a different approach could consist of using a low-order Gauss-Legendre quadrature over the cell width Δ , but this will significantly increase the amount of trajectory storage and, more importantly, the numerical effort during the sweep. Instead, we have chosen to use a few-term Taylor expansion for the exponential and write

$$T \sim e^{-\Sigma \bar{R}_k} \sum_{p=1}^{n_k} \alpha_p \Sigma^p, \quad (8)$$

where \bar{R}_k is the mean chord length within the region and the

$$\alpha_p = \frac{(-1)^p}{p! \Delta} \int_{I_k} [R(x_{\perp}) - \bar{R}_k]^p dx_{\perp}$$

and the value of \bar{R}_k are computed by Gauss-Legendre quadrature during the tracking step. Formula (8) gives accurate values for a small expansion order n_k , while adding a few operations to the track sweep. It requires the storage of $1 + n_k$ coefficients per track, but the calculation of these coefficients, although needing extra local tracking, is done during the tracking step and, therefore, does not have a significant impact in the overall cost of the flux calculation.

The application of the above technique requires that the trajectory band does not encounter any media discontinuity on its path. The easiest way to achieve this is to project all the discontinuities over the transverse direction. However, we have already pointed out that this global projection results on an unnecessarily large number of narrow mesh cells that makes routine calculation prohibitive. Our solution for this dilemma is to use local discontinuity projection and only when necessary. The implementation is done by dividing the trajectory band of every transverse mesh cell, that we call a macroband, into sections. By section we mean the portion of the macroband contained within two consecutive full region crossings (or by boundary surfaces). It is only within each section that we identify and project the discontinuities. An illustration of a section is shown in Figure 2.

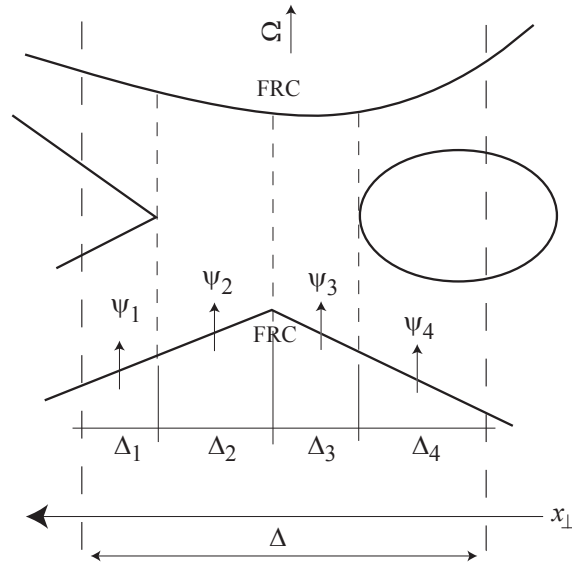


Figure 2. A section within a macroband of width Δ . The section is the area of the macroband between two consecutive full-region crossings (FRC). Only the discontinuities within the macroband are projected within the section to decompose the macroband into four homogeneous sub bands.

For the example shown in the figure, the section of the macroband contains two partially inserted discontinuities plus one boundary discontinuity. Projection over the transverse direction divides the macroband, within the section, into four homogeneous sub bands. The individual fluxes entering each homogenous sub band are propagated via Eq. (5) with the average transmission given by approximation (8). The fluxes ψ_k entering the different homogeneous sub bands of the section are computed from flux continuity, by assuming that the flux $\psi_{upstream}$ exiting the upstream section is constant within the homogeneous sub bands of that section. This gives the following formula:

$$\psi_k = \sum_{k'} \frac{\Delta_{kk'}}{\Delta_k} (\psi_{k'})_{upstream}, \quad (9)$$

where the sum in k' is over all the continuous sub bands contained in the segment upstream and $\Delta_{kk'}$ denotes the length of the intersection of sub band k with sub band k' of the upstream section. The drawback of this approximation is that it generates numerical dispersion across the sections of a macroband, but not across the macrobands. The ψ_k values for the initial section are obtained from the boundary fluxes. The coefficients $\Delta_{kk'}/\Delta_k$ are computed during the tracking phase and added to the tracking trajectory data.

As shown in the following section, to equivalent precision in the results, our technique allows for a band width Δ greater than that required for the classical MOC transverse quadrature and, therefore, for a more efficient calculation. A supplementary advantage is that the technique permits a straightforward implementation for cyclic trajectories, as shown in the appendix.

To summarize:

1. For each direction Ω in the angular quadrature formula, we define a transverse quadrature mesh of

cell width Δ .

2. We decompose the trajectory macrobands defined by each transverse mesh cell into sections. Each section is a part of the trajectory macroband contained within two consecutive full region crossings.
3. By local projection of the discontinuities, each section is decomposed into one or more continuous sub bands.
4. Flux propagation along each homogeneous sub band is calculated with the average transmission given by approximation (8).
5. Equation (9) is used at section interfaces to ensure neutron conservation.

4. NUMERICAL RESULTS

We have implemented the new transverse quadrature technique in a characteristic solver and present here some of the results obtained for different geometry configurations. When not otherwise specified, the results presented below used a Taylor expansion of order $n_k = 5$ in Eq. (8). Because the macrobands in our technique are composed of heterogeneous sections and each section may contain more than one track, to establish a fair comparison with the approximation used in the classical MOC we convert our tracking step Δ into an effective tracking step:

$$\Delta_{eff} = \frac{\Delta}{n_{sb}},$$

where n_{sb} is the average number of homogeneous sub bands within a section. In all our results we used the effective tracking step Δ_{eff} to compare the new technique with classical MOC with step Δ .

4.1. Convergence

We consider first the simple fuel cell in Fig. 3(a) with a uniform source in the moderator. The relative errors in the absorption rate versus the tracking step (Δ for classical MOC and Δ_{eff} for the new technique) are given in Fig. 3(b). We observe that classical MOC exhibits nonuniform convergence, as a result of partial region intersections with trajectory bands. On the other hand, the new technique converges monotonously even for large tracking steps.

4.2. Accuracy

A numerical comparison is given in Table I. We observe that for the same transverse band size the macroband technique is up to six times more accurate than the classical MOC. Conversely, for a given precision, the macroband method allows for a tracking step up to five times larger than classical MOC. For example, to obtain the same precision as in a regular MOC calculation with $\Delta = 0.2 \text{ mm}$, the tracking step with macrobands could be increased up to 1 mm .

These results scale to larger cases. Figures 4 and 5 show a comparison between the classical and the new transverse quadrature techniques over domains with about 500 regions for a typical RBMK cell and a typical PWR assembly, respectively. To avoid compensation errors by full domain averaging, we compared here the maximum relative error in the absorption rate per region. As shown in the figures, error compensation due to the large number of regions makes somewhat smoother the convergence of the

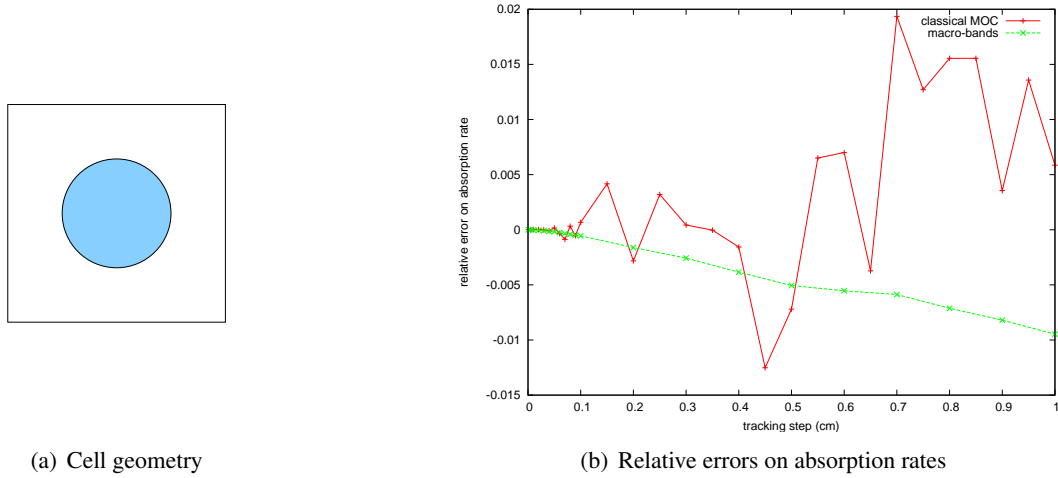


Figure 3. Comparison between the classical MOC and the macroband technique: relative errors for the integrated absorption rate versus tracking step. The reference was classical MOC with 0.005 mm tracking step.

Table I. Relative absorption rate errors versus tracking step as obtained with the classical MOC and the macroband method. The reference used is classical MOC with 0.005 mm tracking step.

tracking step (mm)	0.01	0.05	0.1	0.2	0.5	1
classical MOC	0.00E+00	-6.79E-04	-1.22E-03	-6.40E-03	-8.86E-03	-2.15E-02
macrobands	8.94E-05	-1.07E-04	-4.82E-04	-1.48E-03	-3.48E-03	-3.79E-03

classical MOC. Regardless, the gain in precision with the macroband technique is still significant. For example, a precision of 1% can be obtained with $\Delta_{eff} = 0.1\text{ mm}$, whereas the regular MOC requires $\Delta = 0.025\text{ mm}$ for the same precision.

For the PWR assembly calculation one observes that the averaged number of homogeneous sub bands n_{sb} per section increases with the tracking step Δ . Thus, there is a limit value of Δ beyond which the effective tracking step stagnates (and even decreases) and there is no further improvement of the results.

A final word regarding the sensitivity of the results with respect to the order n_k of the Taylor expansion in Equation (8): figures 4 and 5 show that there is a negligible gain when increasing n_k . Therefore, one could reduce n_k to 1, and even 0, with no appreciable loss in precision. The implication is that, when there is a large number of regions in the geometry domain, the main cause for the error of the classical transverse quadrature is due to the neglect of a correct treatment for regions discontinuities within track bands.

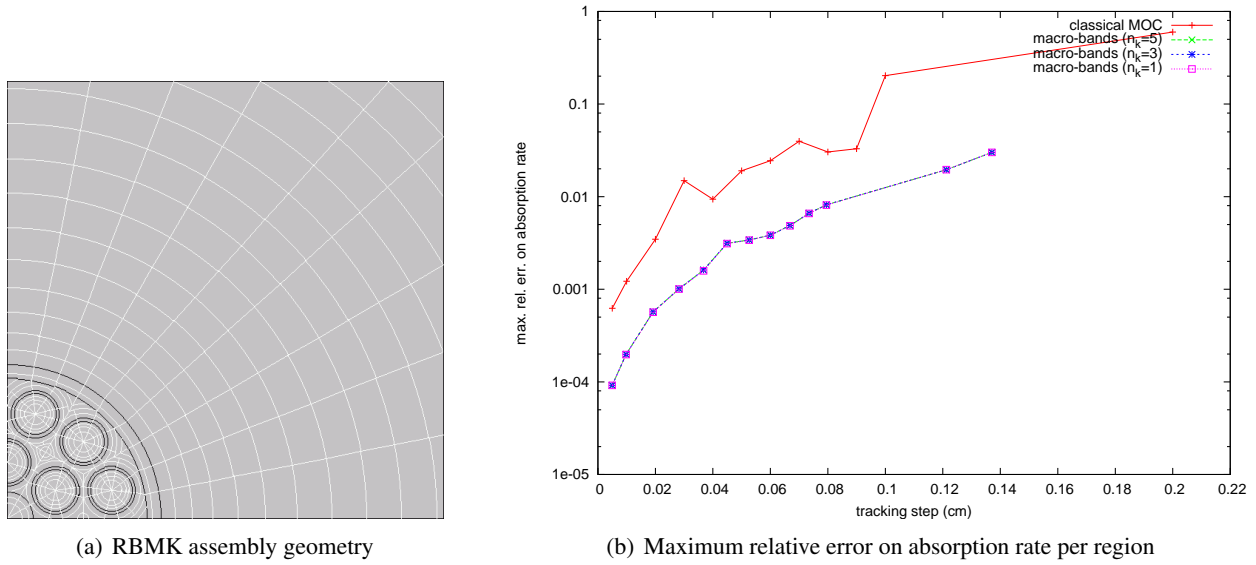


Figure 4. Comparison of the maximum relative errors in the absorption rates per region versus the tracking step for a typical RBMK cell. Results obtained with the classical MOC and the macroband method. The reference is classical MOC with 0.005 mm tracking step.

4.3. Computing Time

Due to the lack of optimization in the implementation of the new transverse quadrature, a direct comparison of computing times with the classical MOC is unfeasible at the time of this writing. Nevertheless, we may compare their algorithmic complexities, both in terms of number of operations and tracking storage requirements. As far as the sweeping is concerned, the move to the macroband technique affects only the treatment of the transmission equation.

The number of arithmetic operations and the size of the tracking data required per track sweep for the macroband and the classical tracking techniques, based, respectively, on Eq. (7) and on Eqs. (8) and (9), are compared in Table II.

Table II. Algorithmic complexities for the classical MOC and the new transverse quadrature method (for $n_k > 1$). r represents the average cost for flux repartition at section interfaces.

tracking technique	exponentials	multiplications	additions	tracking storage
classical MOC	1	2	2	1
macrobands	1	$3 + n_k + r$	$2 + n_k$	$1 + n_k + 2r$

For $n_k = 0$ both techniques are identical, with the exception that the macroband methods adds the extra cost for flux redistribution.

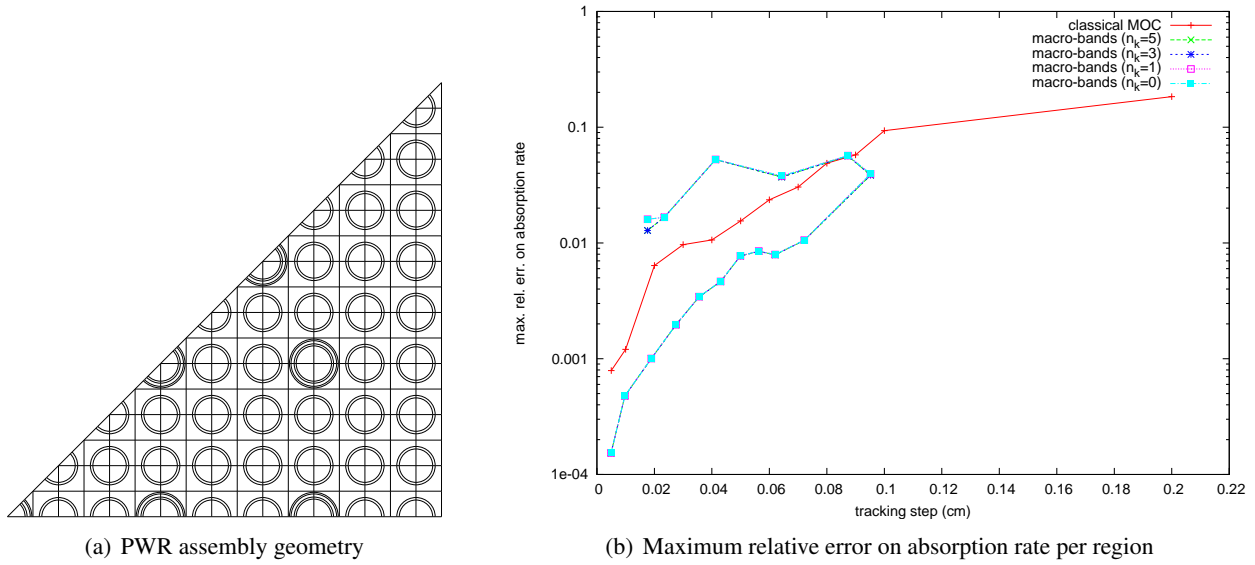


Figure 5. Comparison of the maximum relative errors in the absorption rates per region versus the tracking step for a typical rodged PWR assembly. Results obtained with the classical MOC and the macroband method. The reference is classical MOC with 0.005 mm tracking step.

Because of its dependence on the regions shape and distribution throughout the domain, we are unable to predict the exact value for the average computing cost r for flux redistribution. However, we can evaluate it *a posteriori*, for a particular problem as:

$$r = \frac{\bar{n}_{sb}}{\bar{n}_{reg}}, \quad (10)$$

where \bar{n}_{sb} is the average number of homogenous sub bands per section, and \bar{n}_{reg} is the average number of regions intersecting a homogeneous sub band. A conservative value for the RBMK cell calculation shown in figure 4 is $r \simeq 0.6$. This implies that with a first-order Taylor expansion the new technique requires roughly 2.3 times the amount of operations and 3.2 times the amount of storage needed by the classical MOC with the same tracking step Δ .

5. CONCLUSIONS AND PERSPECTIVES

We have developed and implemented a new tracking technique for the method of characteristics that accounts for material discontinuities and uses a semi-analytical transverse quadrature formula. The observed gain in precision compared to the classical MOC tracking confirms that it is the low precision of the classical transverse integration that severely limits the accuracy of the MOC.

Our numerical examples show that macroband transverse quadrature gives equivalent results than the classical MOC with tracking steps up to 5 times greater. It also guarantees monotonous convergence, even for large values of the tracking step. A comparison of numerical cost and tracking storage requirements shows promise that, with a properly optimized implementation, the macroband method can be nearly twice as fast as the classical MOC.

Still, there remains the error introduced by the piecewise constant approximation for the transverse variation of the angular flux. In future research we intend to investigate the use of a piecewise linear flux

transverse expansion. The combination of this improved flux expansion with the macroband tracking technique introduced in this work has potential for a further increase of the tracking step Δ for a given accuracy.

REFERENCES

- [1] N. Z. Cho, “Fundamentals and Recent Developments of Reactor Physics Methods,” *Nuclear Science and Technology*, **37**, pp. 25-78 (2005)
- [2] M. J. Halsall, “CACTUS, a Characteristics Solution to the Neutron Transport Equations in Complicated Geometries,” *AEEW-R 1291*, Atomic Energy Establishment, Winfrith, Dorchester, Dorset, United Kingdom (1980)
- [3] S. G. Hong and N. Z. Cho, “CRX: a Code for Rectangular and Hexagonal Lattices Based on the Method of Characteristics,” *Annals of Nuclear Energy*, **25**, pp. 547-565 (1998)
- [4] R. Sanchez, L. Mao and S. Santandrea, “Treatment of Boundary Conditions in Trajectory-Based Deterministic Transport Methods,” *Nuclear Science and Engineering*, **140**, pp. 23-50 (2002)
- [5] R. Sanchez, J. Mondot, Z. Stankovski, A. Cossic and I. Zmijarevic, “APOLLO II: a User-Oriented, Portable, Modular Code for Multigroup Transport Assembly Calculations,” *Nuclear Science and Engineering*, **100**, p. 352 (1988)
- [6] K. S. Smith and J. D. Rhodes, “CASMO-4 Characteristics Methods for Two-Dimensional PWR and BWR Core Simulations,” *Trans. Am. Nucl. Soc.*, **83**, pp. 294-296 (2000)
- [7] A. Yamamoto, M. Tabushi, N. Sugimura and T. Ushio, “Non-Equidistant Ray Tracing for the Method of Characteristics,” *Proceedings of M&C 2005*, Avignon, France, September 12–15, 2005

Appendix: MacroBand Tracking in Closed Domains

A geometric domain that fills the entire space by successive replications (boundary translations, rotations or symmetries) requires cyclic tracking in order to obtain the fluxes entering the domain. In this appendix we outline the extension of the macroband tracking technique to deal with this case.

Cyclic tracking uses particular tracking directions and the transverse tracking for each direction is not done over the full projection of the domain on the transverse direction but over a portion of it (see [4]), that we shall call the effective tracking band. For example, for a rectangular domain of dimensions $a \times b$ with translation boundary conditions, the cyclic tracking angles ϕ (angle of the projection of direction Ω on the XY plane with the x axis) and the effective tracking band w are given by the formulas:

$$\begin{aligned} \exists(m, n) \in \mathbb{N}^2 \text{ such that:} \\ \tan \phi &= \frac{m b}{n a}, \\ w &= \frac{a}{m}. \end{aligned} \tag{11}$$

Therefore, one could cover the effective tracking band with K macrobands of width $\Delta = w/K$. However, in this case we have to make sure that the macrobands do not contain a vertex of the domain boundary. This requires the additional constraint that the transverse projections of the vertices of the domain boundary must belong to the transverse mesh that defines the macrobands. The example shown in Fig. 6 shows the

case of the rectangle with translation boundary conditions for the tracking angle defined by $m = 2$ and $n = 1$, as well as the corresponding effective band width. The set of trajectories defined by the band width covers under translations the original rectangle. In the case shown in the figure there is only one vertex along the effective band width in gray and the vertex projection lays on the boundary of the effective tracking band (that covers the left side of the cell). However, it is possible (see [4]) to adopt any band width that has the same area but not exactly on the same position, as illustrated by the dashed lines in Fig. 6. In this case, the vertex projection lies within the tracking domain and must necessarily be part of the transverse tracking mesh. When possible, a careful implementation may select an effective tracking band for which all the vertices projections are on the boundary of effective tracking band and do not constrain the transverse tracking mesh.

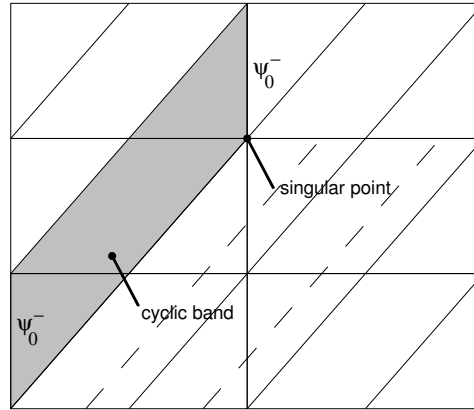


Figure 6. Effective tracking band (in gray) for the case of a rectangle for a cyclic angle with $m = 2$ and $n = 3$ in Eq. (11). The diagonal lines show the direction of projection for the vertices of the geometric domain. An equivalent effective tracking band is also shown by the dashes lines.

Next, consider a cyclic macroband with its sections numbered in increasing order starting with the initial section at the entering boundary. The fluxes exiting the k 'th homogeneous sub band of a section are given by Eq. (5):

$$\psi_k^+ = \underbrace{\prod_i T_{k,i}}_{T_k} \psi_{k,i}^- + \underbrace{\sum_i \frac{1 - T_{k,i}}{\Sigma_i} q_i \prod_{i' > i} T_{k,i'}}_{Q_k} \quad (12)$$

where the sum in i is over the consecutive regions that intersect homogeneous sub band k and $T_{k,i}$ is the transmission integral of sub band k across region i .

As indicated in Eq. 9, the fluxes entering the following section of the macroband are obtained by flux redistribution. By denoting by ψ_s^+ the vector containing the fluxes exiting section s we have

$$\begin{aligned} \psi_{s+1}^- &= R_s \psi_s^+ \\ &= R_s T_s \psi_s^- + R_s Q_s, \end{aligned}$$

where R_s represents the redistribution matrix implicitly defined in Eq. 9, $T_s = \text{diag}\{T_k\}$ is the transmission matrix within section s and Q_s stands for the sources in the different regions within the section.

As for classical cyclic tracking we can recover the entering fluxes from the expression for the fluxes exiting the last section of the macroband:

$$\psi_{in} = T \psi_{in} + Q, \quad (13)$$

where T and Q represent, respectively, the global transmission and source terms for the entire cyclic sweep over the macroband:

$$T = \prod_s R_s T_s,$$

$$Q = \sum_s \prod_{s' > s} R_{s'} Q_{s'}.$$

Matrix T and vector Q can be computed carrying out a sweep of the macroband with a unit entering flux. Then, we use (13) to determine the entering fluxes and effectuate a new sweep to determine the final fluxes.

The computation of T involves matrices of variable size (up to the maximum number of sub bands per section). However, the first and last flux redistribution matrices guarantee that T ends up being a $n \times n$ matrix, where n represents the number of sub bands in the first section. Likewise, the computation of Q involves matrices of different size, but the size of Q is n .